

**Sua Pan Surface Bidirectional Reflectance: A Validation
Experiment of the Multi-angle Imaging
SpectroRadiometer (MISR) During SAFARI 2000**

**Wedad A. Abdou, Stuart H. Pilorz, Mark C. Helmlinger, David J. Diner,
James E. Conel, and John V. Martonchik**

Jet Propulsion Laboratory, California Institute of Technology, Pasadena, CA 91109.

Charles K. Gatebe and Michael D. King

NASA/GSFC, Greenbelt, MD 20771.

Peter V. Hobbs

Atmospheric Sciences Department
University of Washington, Seattle, WA 98195.

Abstract: The Southern Africa Regional Science Initiative (SAFARI 2000) dry season campaign was carried out during August and September 2000 at the peak of biomass burning. The intensive ground-based and airborne measurements in this campaign provided a unique opportunity to validate space sensors, such as the Multi-angle Imaging SpectroRadiometer (MISR), onboard NASA's EOS Terra platform. The MISR validation team participated with a suite of ground-based instruments, including the Portable Apparatus for Rapid Acquisition of Bidirectional Observations of Land and Atmosphere (PARABOLA III) and sun radiometers, to measure the surface bidirectional reflectance and atmospheric aerosol. A participating airborne sensor was the Cloud Absorption Radiometer (CAR) flown onboard the University of Washington's Convair-580 research aircraft. In the absence of clouds, the CAR observations provides measurements of the surface bidirectional reflectance (BRF). This paper presents the first validation study of MISR surface products by comparing MISR retrieval of the surface BRF, at Sua Pan, Botswana, with those evaluated on the ground and from the air, using the PARABOLA and CAR observations, respectively. Two data sets are used in this study; one was collected under clear atmospheric conditions on August 27, and the other, on September 3, exhibited hazy conditions due to several grass fires near Sua Pan. The presence of haze and smoke on September 3 provided a case study to evaluate MISR aerosol retrievals by comparing them with in situ measurements of the aerosol scattering coefficient and particle size distributions obtained aboard the Convair-580 aircraft.

1. Overview

The Multi-angle Imaging SpectroRadiometer (MISR) was launched on December 18, 1999, into a 705-km sun-synchronous Earth orbit aboard the Earth Observing System (EOS) Terra spacecraft. The MISR instrument [Diner *et al.*, 1998] has nine Charge Couple Device (CCD) pushbroom cameras that view the Earth's surface in four spectral bands centered at 446, 558, 672 and 866 nm, and at angles of 0° (A_n), $\pm 26.1^\circ$ (A_f , A_a), $\pm 45.6^\circ$ (B_f , B_a), $\pm 60.0^\circ$ (C_f , C_a) and $\pm 70.5^\circ$ (D_f , D_a), relative to nadir, both forward (+) and aft (-) along the direction of flight. The major science goal of EOS and of MISR is to provide well-calibrated and validated measurements of key parameters that are crucial to the long-term assessment of temporal variations in the Earth radiation budget especially those due to clouds, aerosols, and land surface albedo. The MISR data products provide information on atmospheric aerosol (e.g., optical depth, column-averaged particle size distribution and scattering coefficient) the surface bidirectional reflectance factor (BRF) and the hemispherical directional reflectance factor (HDRF). The BRF is an inherent directional reflectance properties of the surface, defined as the ratio of the radiance reflected by the target surface in a specific direction to that reflected in the same direction by a perfect diffuse (Lambertian) surface under the same collimated beam illumination (i.e., in the absence of an atmosphere) [Matonchik *et al.*, 2000; Nicodemus *et al.*, 1977]. The integration of the BRF over view angles provides the spectral directional-hemispherical reflectance (DHR) of the surface (i.e., the surface spectral albedo). Similarly, the HDRF characterizes the angular reflectance properties of the surface but under ambient illumination, hence its dependency on atmospheric conditions. The integration of the HDRF over view angles provides the bihemispherical reflectance (BHR), defined as the ratio of the radiant exitance to the irradiance of the surface. Knowledge of surface albedos on is crucial to

the understanding of the radiative processes that govern the Sun-Earth system and, therefore, to the assessment of the Earth radiation budget.

The Southern Africa Regional Science Initiative (SAFARI 2000) dry season field study, carried out in the year 2000 during August and September, provided an opportunity to validate the EOS sensors. In that campaign, a wide range of intensive ground- and airborne-based measurements were coordinated during Terra overpasses [King et al., 2002; Swap et al., 2002]. The MISR team participated with a suite of ground-field instruments to acquire surface and aerosol measurements at several sites during the SAFARI campaign. Additionally, simultaneous and colocated airborne measurements were made by other campaign participants. Some of these ground and aircraft measurements are employed in the present study to validate MISR BRF retrievals.

The MISR surface retrieval algorithm begins with the radiative transfer equation [Chandrasekhar, 1960] which describes the observed top-of-atmosphere (TOA) radiance as the sum of three components. The first is due to atmospheric absorption and scattering of the solar radiance without surface interactions; the second and third components involve single and multiple atmosphere-surface interactions, respectively. Consequently, the surface retrieval algorithm requires prior knowledge of the atmospheric parameters. With these parameters determined from the MISR aerosol retrieval process, an iterative technique is used to solve for the surface parameters [Martonchik et al., 1998a]. The strategy is to retrieve the surface HDRF/BHR first, then it is straightforward to obtain the BRF/DHR by removing the effects of the diffuse sunlight and assuming a parameterized BRF [Rahman et al., 1993]. For details of the MISR surface retrieval methodology, see Martonchik et al., [1998a].

The MISR aerosol retrieval algorithm [Martonchik *et al.*, 1998b] is based on a procedure that does not require knowledge of the absolute surface reflectance or its spectral characteristics. The main assumption is that the surface-leaving signal is angular in shape and spectrally invariant. The MISR multi-angle viewing strategy enhances the aerosol signal as the atmospheric path length increases with view angles. This helps establish a representation of the angular shape of the surface component of the observed radiances using empirical orthogonal functions (EOFs). The aerosol properties are then derived from fitting the angular shape of the remaining signal to modeled atmospheric path radiances. The latter are simulated for a set of preselected aerosol mixtures, each containing a maximum of three pure particle types in specified proportions. Simultaneous solutions are then determined for the coefficients of the dominant surface EOFs and for the aerosol column optical depth associated with the TOA path radiance used in the retrieval attempt. Successful retrievals are those for which the mean-squared differences, χ^2 , between observations and simulated radiances are smaller than a specified threshold. The best fit-model is that which corresponds to the minimum value for χ^2 . The mean optical depth, averaged over all possible models, is then used for the final retrieval of the surface products.

Two data sets obtained at Sua Pan, Botswana (20.6° S, 26.1° E) on August 27 and September 3, 2000, were selected for this study. On these two days, at ~0852 UTC (~1052 local time), MISR passed over Sua Pan, on orbits 3684 (path 172, block 107) and 3786 (path 173, block 107), respectively. The MISR images of Sua Pan indicate, as shown in Figure 1, clear atmospheric conditions on August 27, and thick haze and smoke on September 3, due to wild and man-made grass fires that erupted earlier at several spots near Sua Pan. This large difference in aerosol loading

provides an opportunity to evaluate the effect of the MISR atmospheric correction process on retrieving the surface BRDF. In-situ airborne aerosol measurements made over Sua Pan are used to help in this evaluation.

2. Surface BRDF measurements and results

The MISR validation team was present at Sua Pan from August 24 to September 4, 2000, and made daily measurements of the surface directional reflectance using *the Portable Apparatus for Rapid Acquisition of Bidirectional Observations of Land and Atmosphere (PARABOLA) version III*. This instrument [Bruegge *et al.*, 2000] provides complete hemispherical scans of the sky downwelling and surface upwelling radiances, on a 5° spherical grid, in eight spectral bands, centered at 444, 551, 650, 860, 944, 1028, 1650, and 533 (400 -700) nm. The surface BRDF is retrieved from the PARABOLA data using a methodology that requires measurements over a range of solar angles, preferably from sunrise to noon or from noon to sunset [Martonchik, 1994]. The PARABOLA was set-up early every morning and observations were made at a fixed location from sunrise to noon, including the time during Terra overpass (\sim 1052 local time). The retrieval process of surface directional reflectance from PARABOLA data is described by Abdou *et al.*, [2000].

Sua Pan, one of the salt pans northeast of Botswana, is about 3500 km² of desert-like surface surrounded by grasslands. The pan surface is mainly salt mixed with clay and dust. The top layer is loose and dusty particles come-off the pan in presence of strong winds. Tracks are easily made due to people and vehicles moving on the pan exposing relatively darker layers just beneath the

top surface. An example of the BRF retrieved from the PARABOLA data on August 27 is shown in Figure 2. This polar plot shows an almost diffuse surface with no strong angular signatures. The surface BRF has its minimum values on the horizon in the forward direction and increases gradually to maximum values in the backscattering direction. A diffuse “hot spot” is increasingly obvious at larger wavelengths but appears shifted from the anti-solar point, in this case at $\sim 35^\circ$.

The presence of small scale inhomogeneities in surface brightness were evident to the MISR field engineers. Meaningful comparison of air- or space-borne observations with the ground measurements are possible only when such inhomogeneities are considered and properly averaged out in the ground measurements. To determine the range in brightness on the pan surface, MISR team members used the *portable spectrometer manufactured by Analytical Spectral Devices (ASD)*. This instrument provides measurements of the surface HDRF in the nadir direction and over the spectral range 350 to 2500 nm. This is done by alternately measuring the radiance reflected from the target surface and that reflected from a reference lambertian surface, in this case a Spectralon panel. The surface HDRF is determined by the ratio of the two radiances. The portable ASD provided rapid HDRF measurements over a large area surrounding the PARABOLA without significant changes in the illumination or atmospheric conditions during the Terra overpass time. A Global Positioning System (GPS) was used to record the latitude and longitude of the locations where the ASD measurements were obtained. Figure 3 illustrates the range of the HDRF values measured by the ASD at various locations on the pan surface. The BRF at a given location on the pan is determined by normalizing the PARABOLA data at nadir by the ASD data at that location. The PARABOLA together with the ASD measurements provide the BRF within ~ 2 to 3% accu-

racy at solar and view angles smaller than $\sim 45^\circ$ and within $\sim 8\%$ at more oblique angles. In the present analyses, an upper limit of 10% uncertainty is assumed.

Additionally, simultaneous and co-located BRF measurements were made with *The Cloud Absorption Radiometer (CAR)* that flew aboard the University of Washington Convair CV-580 research aircraft over Sua Pan on September 3 [Hobbs, 2003]. The CAR is an airborne multispectral scanning radiometer developed at Goddard Space Flight Center originally for the study of cloud absorption [King *et al.*, 1986]. The instrument is designed to scan the sky downwelling and the ground upwelling radiances from zenith to nadir in 1° field of view in 14 spectral channels (340-2300 nm). The multiangle viewing geometry of the CAR allows determination of the directional reflectance properties of terrestrial surfaces [Tsay *et al.*, 1998; Soulen *et al.*, 2000; Gatebe *et al.*, 2001]. As the Convair-580 flew in ~ 3 km circles at 600 m altitude above the Sua Pan, the CAR made several complete orbital measurements that extended from 0949 to 1000 UTC at a solar zenith angle of $\sim 28.5^\circ$. At 600 m altitude, the resolution of the CAR is ~ 10 m at nadir and ~ 270 m at 80° view angle. The surface BRF was retrieved from the CAR measurements after applying an atmospheric correction to remove the radiances scattered by the ambient atmosphere [Gatebe *et al.*, 2002]. The ground and airborne BRFs were interpolated to MISR wavelengths and viewing geometries, given in Table 1, and compared with the values retrieved from MISR data on August 27 and September 3, as shown in Figures 4 and 5, respectively (on August 27 the Convair-580 did not fly over the Sua Pan).

As shown in Figure 4, the MISR data on August 27 agree to better than 10% with the ground-based BRF for the near-nadir angles in all the spectral bands and in the most oblique backscatter-

ing view angles in the red and near infrared bands. In the forward scattering, the MISR retrieved BRFs are generally larger than the ground-based values. On September 3, the CAR and PARABOLA data are in very good agreement at all viewing angles and in all the channels. However, on that day the MISR retrieval underestimates the BRF at most view angles and in all channels, more so in the backscattering direction. This disagreement, however, remains within the shaded areas that represent the range of the surface brightness. The disagreements between the MISR and the ground and airborne data could be due in part to uncertainty in co-locations of the data. Geo-registration of MISR images are better than 2 pixels [Jovanovic *et al.*, 1998]. The MISR resolution in the crosstrack is 275 m for all off-nadir cameras and 250 m for the nadir camera. Downtrack, the resolution ranges from 214 m in the nadir to 707 m in the D cameras. The MISR data used in this work are in the nominal global mode that provides 275 m sampling in all bands of the nadir camera and the red band of each of the off-nadir cameras, and 1.1 km (averaged over 4 x 4 pixels) for the remaining 24 channels. At this resolution, the MISR geo-registration is within 0.5 km near nadir to ~1.5 km at the most oblique view angles. However, using the numerous ASD data at various locations on the pan, and the help of the GPS data that accompanied the ground and aircraft measurements, co-location of the data is a straightforward process and it does not produce the large disagreements shown in Figures 4 and 5. A more plausible source for these disagreements is the uncertainty in the atmospheric correction provided by the MISR aerosol retrieval. This is evaluated in the following section by examining MISR aerosol products and comparing them with some of those made on the ground and from the Convair-580.

3. Aerosol measurements.

The MISR team made several measurements of the aerosol optical depth using *The autotracking Reagan sun-radiometers*. Two of these radiometers were used to measure the incident solar irradiance in 10 spectral channels in the range 380 to 1030 nm. The spectral aerosol and ozone optical depths were determined from these data using the well known Langley technique. The Rayleigh scattering optical depth, required by this technique, is calculated from field measurements of atmospheric pressure. Figure 6 illustrates the aerosol optical depth obtained from the sunphotometers's measurements on August 27 and September 3. The data on September 3 indicate the thick haze and smoke that were present on that day. *The CIMEL sky photometer* was also used to measure light scattering in the solar aureole, as well as in the almucantar and the principal plane. The CIMEL data provide the atmospheric optical depth, but they are used, in addition, to determine the aerosol phase function, single scattering albedo, and particle size distribution using the retrieval algorithm described by *Dubovik and King* [2000]. The CIMEL data on September 3 indicate a relatively absorbing aerosol with a single scattering albedo, ω_0 , of 0.9 and a complex refractive index of $1.44-0.01i$ in the MISR green band. The retrieved particle size distribution, shown in Figure 7, has three modes with characteristic radii of about 0.1, 1.0 and 6.0 μm . No results were available for August 27, but those available on August 28, show a size distribution similar to the one obtained for September 3. The CIMEL results obtained for the SAFARI campaign sites are posted on the AErosol RObotic NETwork (AERONET) website at: <http://aeronet.gsfc.nasa.gov> [*Holben et al., 1998*].

Additionally, *an Integrating 3-wavelength nephelometer and a Particle Measurement System (PMS) model PCASP-100X* were aboard the Convair-580 to measure the vertical profiles of the aerosol light scattering coefficient and particle size distribution over Sua Pan on September 3

[Hoblen, 2003]. Figure 8 compares the insitu particle size distribution with that inverted from the CIMEL ground measurements (henceforth the AERONET data) after converting the later to column number density. Figure 9 illustrates the nephelometer measurements of the particle light scattering coefficient in the red channel, as a function of altitude, during the Terra overpass. The insitu particle size distribution measurements indicate a well mixed aerosol with at least two modes, one at $\sim 0.1 \mu\text{m}$ and the other at $\sim 1.0 \mu\text{m}$ radius. It should be noted that the insitu measurements are sensitive only to particle size in the range 0.06 to $1.5 \mu\text{m}$ in radius, while the AERONET inversion is insensitive to particles below $0.05 \mu\text{m}$. Within these limits, the two independent measurements, shown in Figure 8, are reasonably consistent. Estimates of the light scattering coefficient from the AERONET data are also consistent with the insitu airborne measurements shown in Figure 9. For example, using the retrieved values of 0.58 and 0.89 for the optical depth, τ , and single scattering albedo, ω_0 , in the red channel (672 nm), respectively, and a scale height, H , of 1.8 km , as estimated from the AERONET data, a column-averaged value for the scattering coefficient was estimated to be $\sim 2.6 \times 10^{-4} \text{ m}^{-1}$. The value from the in situ nephelometer measurements shown in Figure 9 is $\sim 2.2 \times 10^{-4} \text{ m}^{-1}$ at 700 nm . Using both the AERONET and insitu data, the column-averaged scattering cross section is estimated to be in the range $\sim 1 \times 10^{-14}$ to $\sim 1 \times 10^{-13} \text{ m}^2$. These values are characteristic of particles much smaller than those indicated from the particle size distributions shown in Figure 8. The dotted line in Figure 8 represents a particle size distribution that contains an extra mode at $r_c = 0.03 \mu\text{m}$. This model, as will be shown later, may be a more realistic representation of the actual aerosol present on September 3.

The MISR aerosol retrievals over the Sua Pan for August 27 and September 3 are shown in Figure 10 and 11 respectively. It is clear from these figures that the retrieved optical depths are not in

good agreements with those measured on the ground. The best-fit model determined for August 27 is one composed of small non-absorbing spherical particles with a log-normal size distribution with characteristic radius, $r_c = 0.03 \mu\text{m}$ and a distribution width, $b = 1.65 \mu\text{m}$. The particle effective radius is $0.056 \mu\text{m}$ and its scattering cross section in the green band is $3.96 \times 10^{-12} \text{m}^2$. As expected with this model, which consists only of small particles, the retrieved optical depth diminishes with wavelength. However, it does so much more steeply than the ground-based measurements of optical depth. As is evident from the spectral behavior of the mean optical depth, successful retrievals were also obtained for larger particles. The mean optical depth, which is used in retrieving the surface BRF, was underestimated in all of the MISR bands. This explains the overestimated values of the MISR BRF in most oblique view angles, as shown in Figure 4. However, it does not explain the underestimated values in the backscattering direction in the blue and green bands.

On September 3, the best-fit aerosol model was a mixture of two pure particles: a white spherical particle with $r_c = 0.12 \mu\text{m}$ and $b = 1.75 \mu\text{m}$ which contributes 85% to the optical depth, and soot with $r_c = 0.012 \mu\text{m}$ and $b = 2$, which contributes 15% to the optical depth. The effective radius of this mixture is $\sim 0.11 \mu\text{m}$, and its effective complex refractive index and single scattering albedo are $1.46 - 0.019i$ and 0.88 , respectively, in MISR's green band. This mixture is close in characteristics to the one retrieved from the CIMEL data. However, the retrieved optical depth values are not in agreement with the ground-based measurements. Except in the blue, the mean optical depth retrieved from MISR on September 3 was overestimated. Again this explains the underestimation of the retrieved BRF in all the bands except in the blue. Since the TOA radiance is directly related to the aerosol phase function, P , and to ω_0 and τ , it is possible that, depending on the scattering

angle, the combined effect of these parameters may result in a smaller or larger aerosol contribution to the TOA radiances and, consequently, increase or decrease in the surface contribution.

It is of interest to find an alternative, or a “preferred” aerosol model that has similar physical and optical properties as the one retrieved from the CIMEL data and which also fit the MISR TOA radiances. The best-fit aerosol model found was a mixture that contains an 85% (by optical depth) of small particles with $r_c = 0.03$ and $b = 1.8$ mixed with 15% of particles with $r_c = 1.0$ and $b = 1.8$. With all particles having the same refractive index of $1.45 - 0.01i$, this model has a single scattering albedo of 0.89 in the green band and a scattering cross section of $1 \times 10^{-11} \text{ m}^2$. As illustrated in Figures 10 and 11, the extinction cross section of this simulated aerosol mixture shows the same spectral behavior of the optical depth measured on August 27 and September 3. Using this best-fit model, and the ground-based measurements of the optical depth and surface BRF, the TOA radiances were estimated in MISR’s viewing geometry (shown in Table 1) and compared with MISR observations on September 3. As shown in Figure 12, the simulated model is a good candidate, but some fine tuning of the model is still required to obtain a better fit.

It is clear that the uncertainties in the MISR BRF retrievals can be explained, for the most part, by errors in retrieving the aerosol type and optical depth. A thorough evaluation, however, requires more data and in-depth analyses of the shape of the phase function and the product $P\omega_0 \tau$, with scattering angles. The MISR science team is currently reviewing the aerosol climatology employed in the aerosol retrieval process in an effort to improve the retrievals of aerosol and surface products from MISR. Aircraft and surface data such as those reported in this paper for Sua Pan, provide valuable data that can help to improve the satellite data analysis.

4. Summary and Conclusion

This paper describes an effort to validate MISR retrievals using ground and airborne measurements that were made at Sua Pan, Botswana, during the SAFARI 2000 dry season campaign. Two sets of data, one on a clear day on August 27 and the other on a hazy day on September 3, were selected to examine the effects of atmospheric correction on the MISR surface retrieval process. The BRDF retrieved from the MISR data were not in good agreements with either the ground or airborne data. The MISR atmospheric correction process was discussed as the primary source of these disagreements. Except for a few view angles, the values of the BRDF retrieved from MISR data have an inverse relation to the optical depths retrieved from the same data. The MISR aerosol climatology, i.e., the preselected set of aerosol mixtures considered in the retrieval process, needs to be reviewed to see if improvements can be made to the retrievals.

Acknowledgments. The authors thank B. N. Holben for making the CIMEL data available on the AERONET site. This study was conducted at the Jet Propulsion Laboratory, California Institute of Technology, under contract with NASA (the National Aeronautics and Space Administration). The University of Washington team was supported by NASA and NSF (the National Science Foundation).

Table 1: MISR viewing Geometry¹ at Sua Pan.

August 27: Sun zenith angle = 37.8°									
Camera	Df	Cf	Bf	Af	An	Aa	Ba	Ca	Da
Zenith viewing	71	61	46	27	4	26	45	60	70
Relative Azimuth ²	159	160	161	165	119	30	27	26	25
Scattering Angle	144	153	165	166	144	119	99	85	75
September 3: Sun zenith angle = 34.6°									
Zenith viewing	70	60	46	27	10	28	46	61	71
Relative Azimuth ²	153	151	146	136	64	26	13	17	19
Scattering Angle	139	147	156	157	140	117	100	86	76
1- All values are rounded to nearest degree.									
2- Relative to Sun azimuth. angle									

REFERENCES

Abdou W. A., M. C. Helmlinger, J. E. Conel, C. J. Bruegge, S. H. Pilorz, J. V. Martonchik, and B. J. Gaitley, Ground measurements of surface BRF and HDRF using PARABOLA III., *J. Geophys. Res.*, 106, 11,967-11,976, 2000.

Bruegge, C. J., M. C. Helmlinger, J. E. Conel, B. J. Gaitley, and W. A. Abdou, PARABOLA III: a sphere-scanning radiometer for field determination of surface anisotropic reflectance functions, *Remote Sens. Rev.*, 19, 75-94, 2000.

Chandrasekhar, S., *Radiative Transfer*, Dover Publication, Inc., New York, 1960.

Diner, D. J, C. J. Bruegge, J. V. Martonchik, T. P. Ackerman, R. Davies, S. A. W. Gerstl, H. R. Gordon, P.J. Sellers, and J. Clark, J. A. Daniels, E. D. Danielson, V. G. Duval, K. P. Klassen, G. W. Lilienthal, D. I. Nakamoto, R. Pagano, and T. H. Reilly, MISR: A Multi-angle Imaging SpectroRadiometer for geophysical and climatological research from EOS, *IEEE Trans. Geosci. and Remote Sens.*, 27, 200-214, 1989.

Dubovik, O. and M. D. King, A flexible inversion algorithm for retrieval of aerosol optical properties from Sun and sky radiance measurements, *J. Geophys. Res.*, 105, 20 673-20 696, 2000.

Gatebe, C. K., M. D. King, S. C. Tsay, Q. Ji, G. T. Arnold and J. Y. Li, Sensitivity of off-nadir zenith angles to correlation between visible and near-infrared reflectance for use in remote sensing of aerosol over land, *IEEE Trans. Geosci. Rem. Sens.* 39, 805-819, 2001.

Gatebe, C. K., M. D. King, S. Platnick, G. T. Arnold, E. F. Vermote, and B. Schmid, Airborne spectral measurements of surface-atmosphere anisotropy for several surface and ecosystem over southern africa, *J. Geophys. Res.*, this issue, 2003.

Hobbs, P. V., Technical Appendix: An overview of the University of Washington's airborne measurements in the SAFARI 2000 field study in southern Africa, *J. Geophys. Res.*, this issue, 2003.

Holben, B. N., T. F. Eck, I. Slutsker, D. Tanre, J. P. Buis, A. Setzer, E. Vermote, J. A. Reagan, Y. Kaufman, T. Nakajima, F. Lavenu, I. Jankowiak, and A. Smirnov, AERONET-A federal instrument network and data archive for aerosol characterization, *Rem. Sens. Environ.*, **66**, 1998.

Jovanovic, V., M. M. Smyth, J. Zong, R. Ando, and G. W. Bothwell, MISR photogrammetric data reduction for geophysical retrievals, *IEEE Trans. Geosci. Remote Sens.*, **36**, 1290-1301, 1998.

King, M. D., S. Platnick, and C. C. Mueller, Remote Sensing of Smoke, Land and Clouds from NASA ER-2 during SAFARI 2000, *J. Geophys. Res.*, this issue, 2002.

King, M. D., M. G. Strange, P. Leone, and L. R. Blaine, Multiwavelength scanning radiometer for airborne measurements of scattered radiation within clouds, *J. Atmos. Oceanic. Tech.*, **3**, 513-522, 1986.

Martonchik, J. V., Carol J. Bruegge, and Alan H. Strahler, A review of reflectance nomenclature used in remote sensing, *Rem. Sens. Rev.*, **19**, 9-20, 2000.

Martonchik, J. V., D. J. Diner, B. Pinty, M. M. Verstrate, R. B. Myneni, Y. Knyazikhin and, H. R. Gordon, Determination of the land and ocean reflective, radiative, and biophysical properties using multiangle imaging, *IEEE Trans. Geosci. Remote Sens.*, 36, 1266-1281, 1998a.

Martonchik, J. V., D. J. Diner, R. Kahn, M. M. Verstrate, B. Pinty, H. R. Gordon, and T. P. Ackerman, Techniques for the retrieval of aerosol properties over land and ocean using multiangle imaging, *IEEE Trans. Geosci. Remote Sens.*, 36, 1212-1227, 1998b.

Martonchik, J. V., Retrieval of surface directional reflectance properties using ground level multi-angle measurements, *Rem. Sens. Environ.*, 50, 303-316, 1994.

Nicodemus, F. E., J. C. Richmond, J. J. Hsia, I. W. Ginsberg, and T. Limperis, Geometric Considerations and Nomenclature for Reflectance, U. S. A. Department of Commerce/ National Bureau of Standards, NBS Monograph, 160, 1-52, 1977.

Rahman, H., B. Pinty, and M. M. Verstraete, Coupled surface-atmosphere reflectance (CSAR) model 2. Semiempirical surface model usable with NOAA Advanced Very High Resolution Radiometer data, *J. Geophys. Res.*, 98, 20791-20801, 1993.

Soulen, P. F., M. D. King, S. C. Tsay, G. T. Arnold, and J. Y. Li, Airborne spectral measurements of surface anisotropy during the SCAR-A, Kuwait oil fire, and TARFOX experiment, *J. Geophys. Res.*, 105, 10203-10218, 2000.

Swap, R. J., H. J. Annegarn, J. T. Suttles, J. Haywood, M. C. Helmlinger, C. Hely, P. V. Hobbs, B. N. Holben, J. Ji, M. D. King, T. Landmann, W. Maenhaut, L. Otter, B. Pak, S. J. Piketh, S. Plattnick, J. Privette, D. Roy, A.M. Thompson, D. Ward, R. Yokelson, The Southern African Regional Science Initiative (SAFARI 2000): Dry-season field campaign: An overview, *South African J. of Sci.*, submitted, 2002.

Tsay, S. C., M. D. King, G. T. Arnold, and J. Y. Li, Airborne spectral measurements of surface anisotropy during SCAR-B, *J. Geophys. Res.*, **103**, 31943-31954, 1998.

Figure Captions

Figure 1. The MISR B_a images of Sua Pan, Botswana, on (a) August 27 and (b) September 3. The “X” marks the location of the ground campaign. The haze shown in (b) is due to smoke from biomass fires that were present near Sua Pan. The relatively clear atmosphere on August 27 was due to the wind conditions, which cleared out the smoke that morning.

Figure 2. A polar plot of the surface BRF retrieved from the PARABOLA measurements at Sua Pan on August 27, 2000, during a Terra overpass.

Figure 3. The surface HDRF as measured by the ASD instrument. The HDRF values represent the range of brightness of the Sua Pan surface.

Figure 4. A comparison of the BRF retrieved from MISR data at Sua Pan on August 27, with those retrieved from the ground-based PARABOLA on the same day. The shaded area represents the range of brightness of the Sua Pan surface.

Figure 5. A comparison of the BRF retrieved from MISR data at Sua Pan on September 3, with those retrieved from the ground-based PARABOLA and the aircraft-based CAR data. The shaded area represents the range of brightness of the pan surface.

Figure 6. The optical depth values measured by the sun-radiometers at Sua Pan, on August 27 and September 3, during a Terra overpass at 0852 UTC.

Figure 7. The aerosol column volume size distribution retrieved (using the Dubovik method) from the CIMEL (AERONET) data at Sua Pan on September 3.

Figure 8. A comparison of the insitu particle size distribution measured by the PMS PCASP-100X aboard the Convair_580 with that retrieved from the CIMEL (AERONET) data. The latter was

derived from the data shown in Figure 7 and represents the column number density. These data were retrieved from measurements that are not sensitive to particles of radii less than $\sim 0.05 \mu\text{m}$.

Figure 9. The particle scattering coefficient retrieved from the in-situ measurements at Sua Pan on September 3.

Figure 10. Aerosol optical depth retrieved from MISR data at Sua Pan on August 27. The dash line represents what is called here “the preferred model” that was simulated to fit the ground-based optical depth measurements as well as the MISR radiances. This best-fit model exhibits the same spectral behavior of the measured optical depth. This is illustrated by the dash line which represents the scattering cross section of the best-fit model scaled to the optical depth.

Figure 11. Same as in Figure 10, but for September 3.

Figure 12. Comparison of the radiances simulated at MISR’s cameras, using the preferred model and the PARABOLA BRF, with MISR radiances at Sua Pan on September 3.

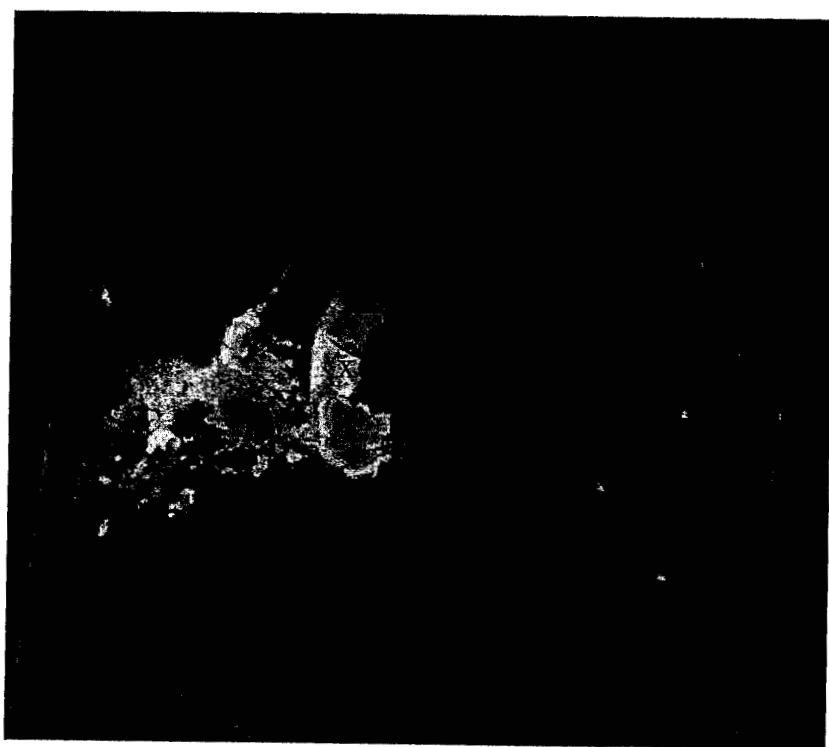


Figure 1a.

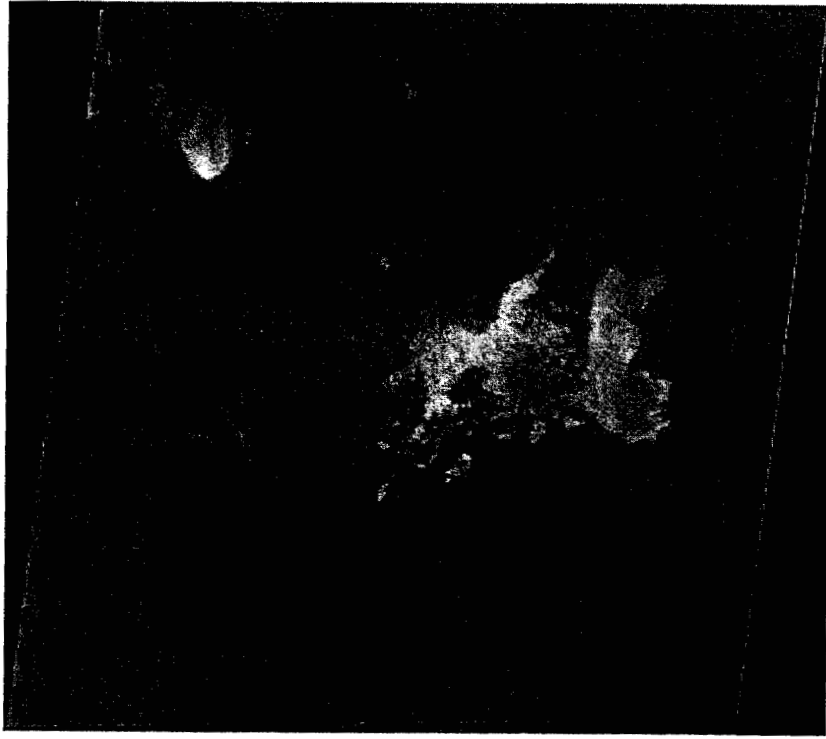


Figure 1b.

BIDIRECTIONAL REFLECTANCE FUNCTION

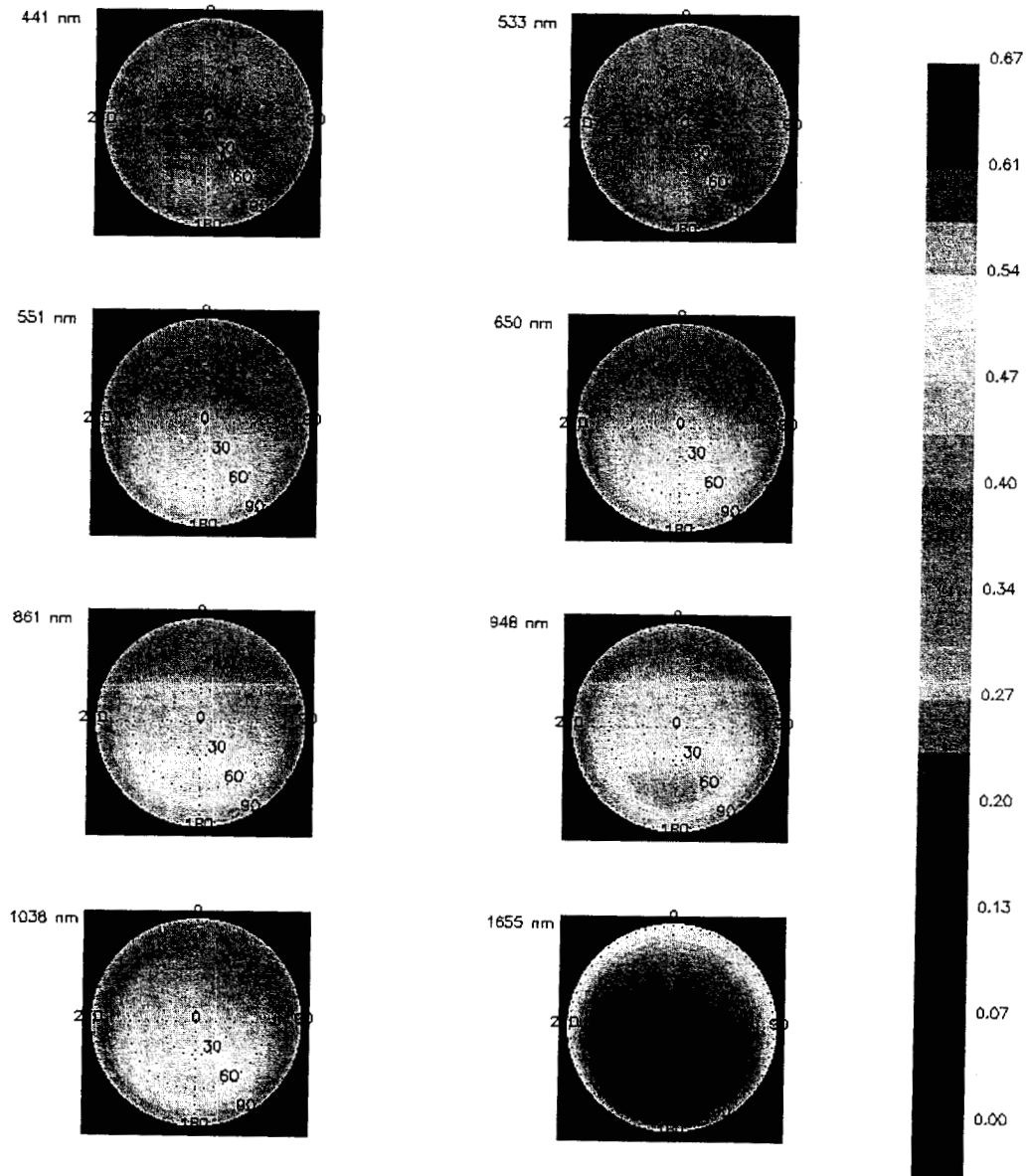


Figure 2.

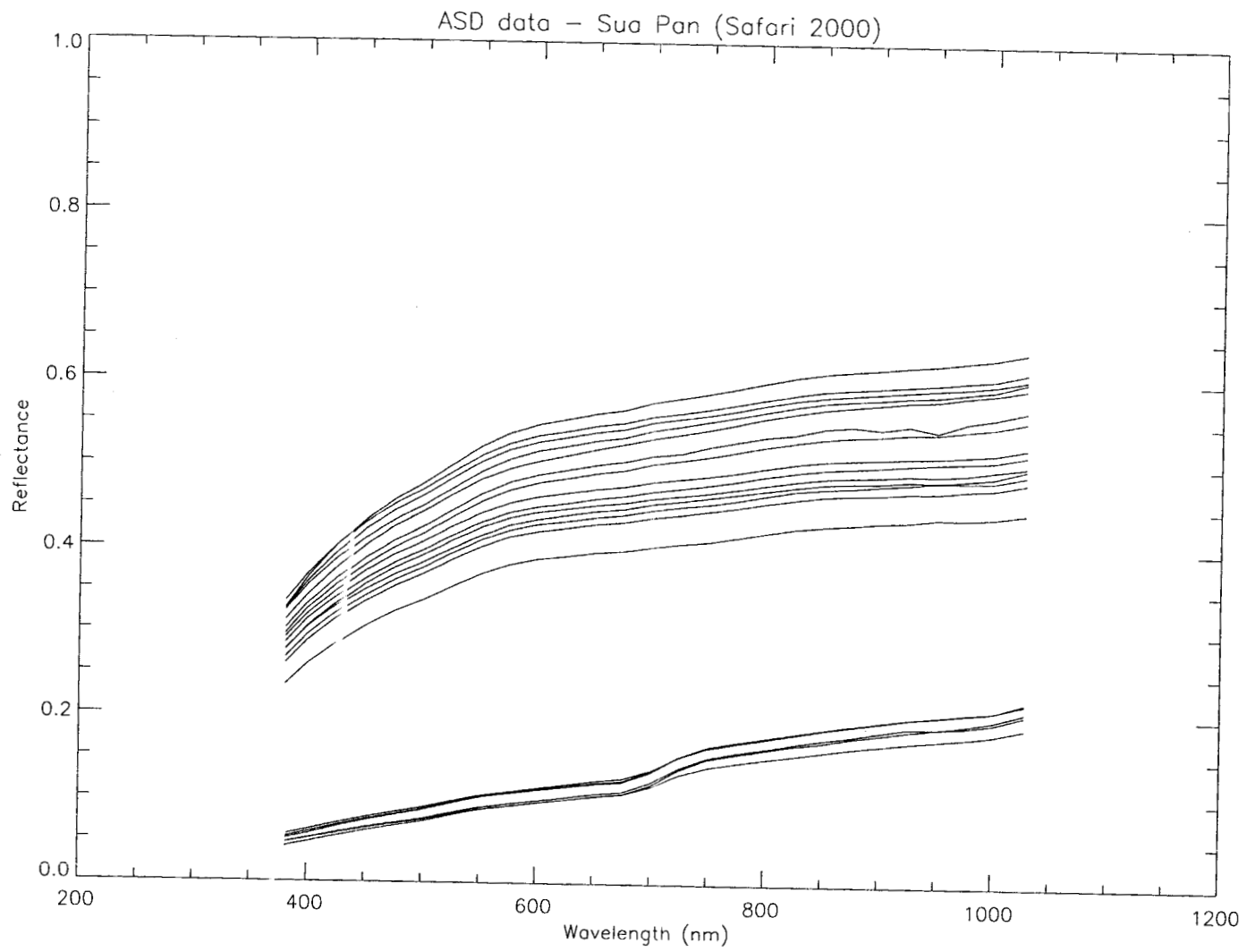


Figure 3.

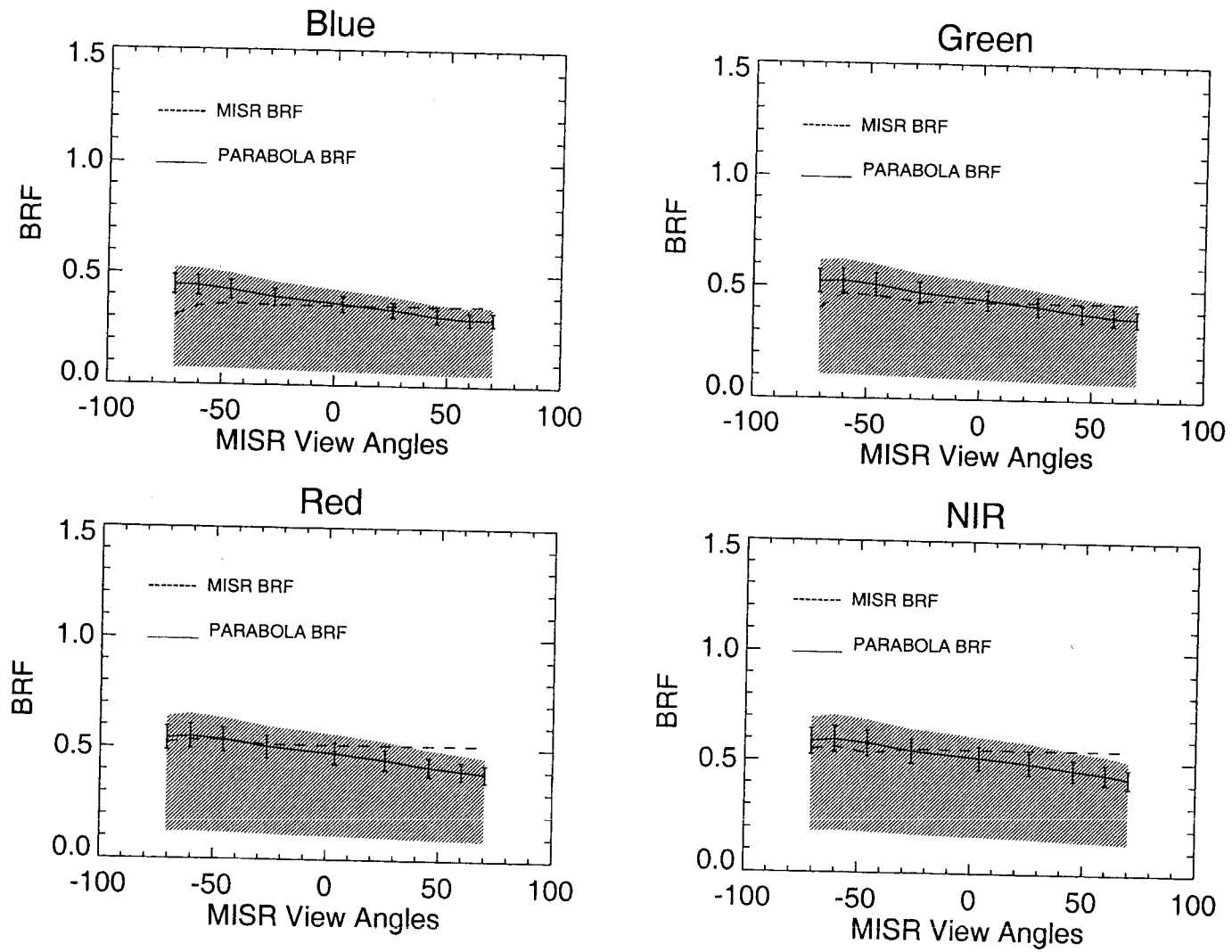


Figure 4.

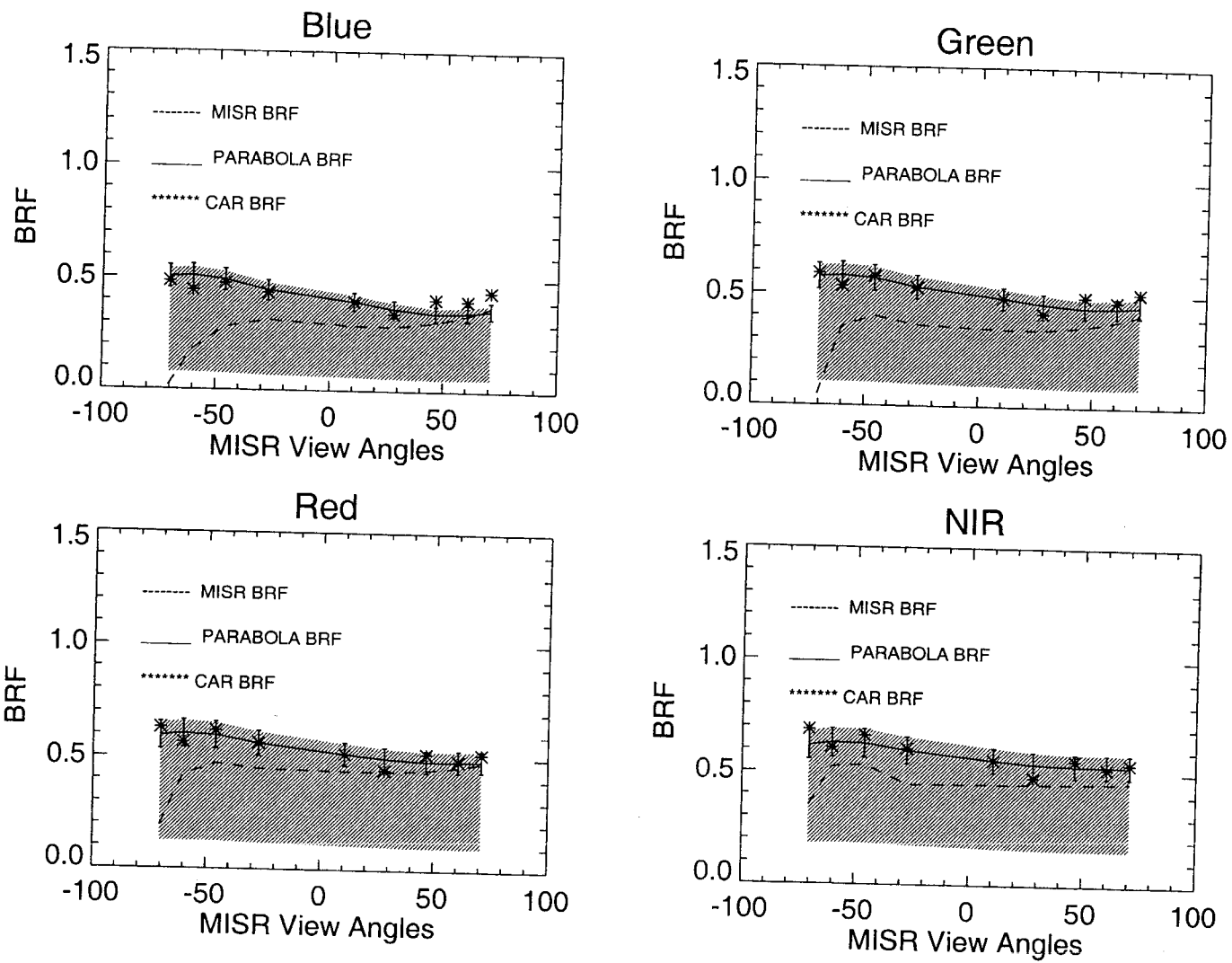


Figure 5.

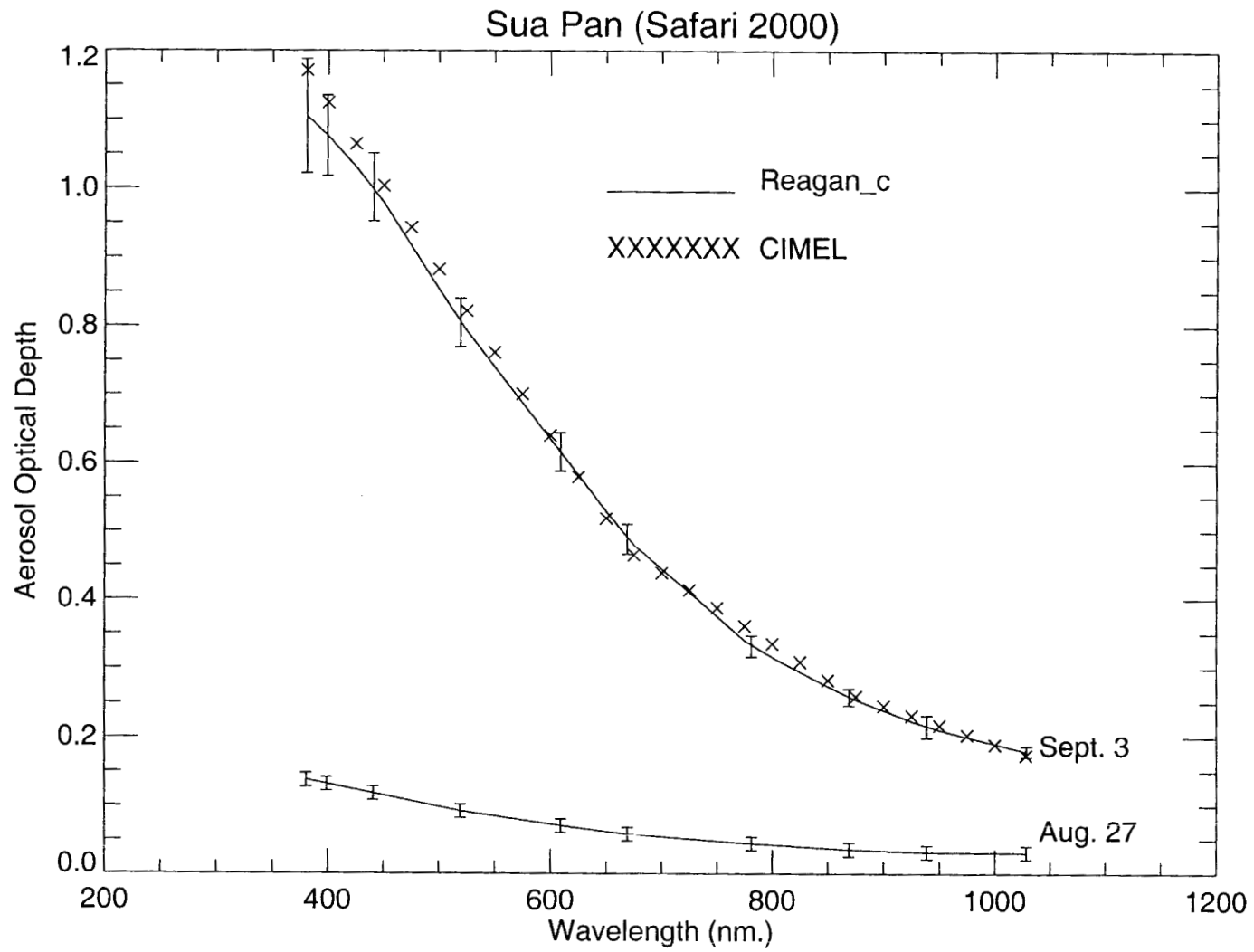


Figure 6.

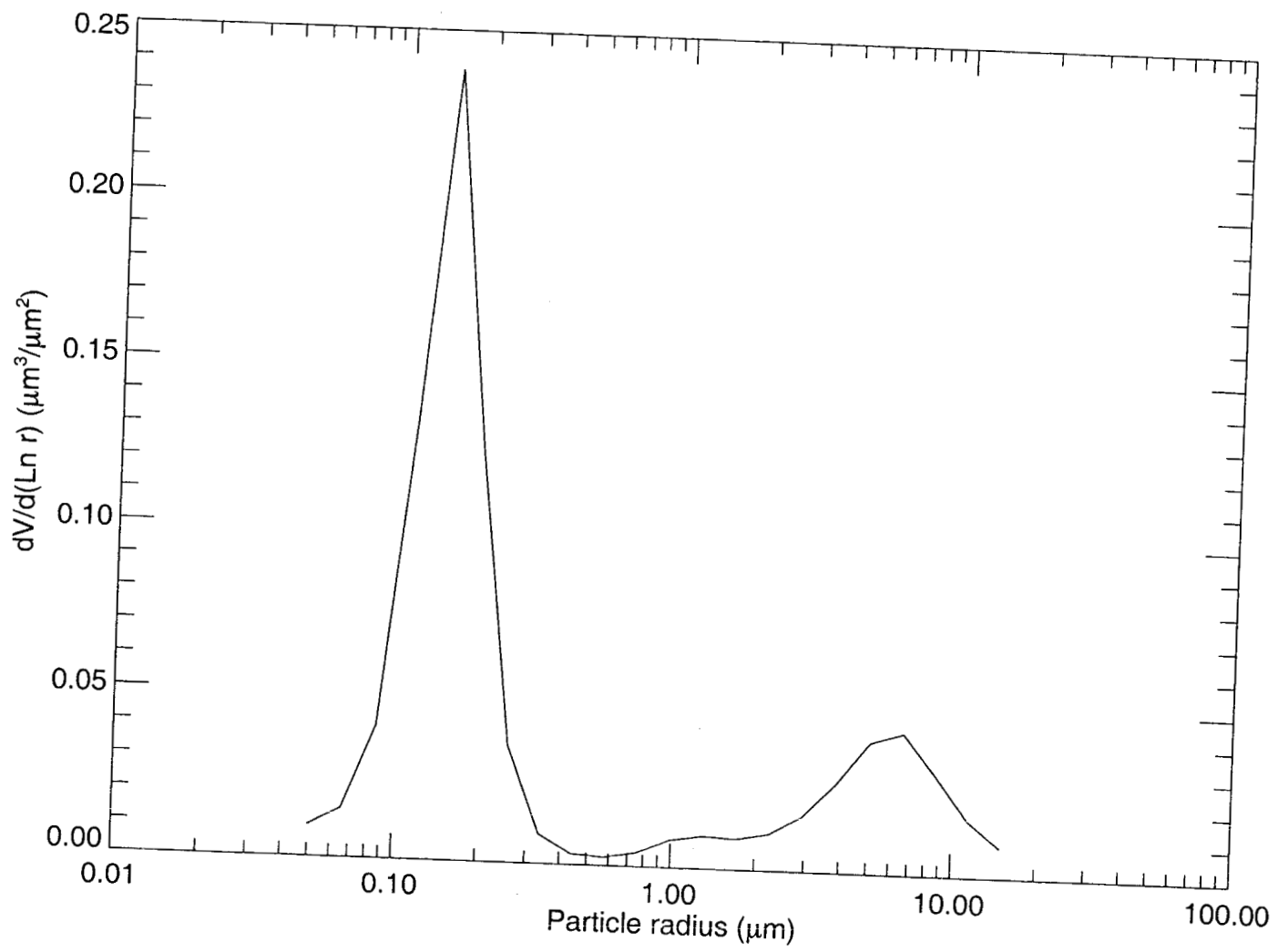


Figure 7.

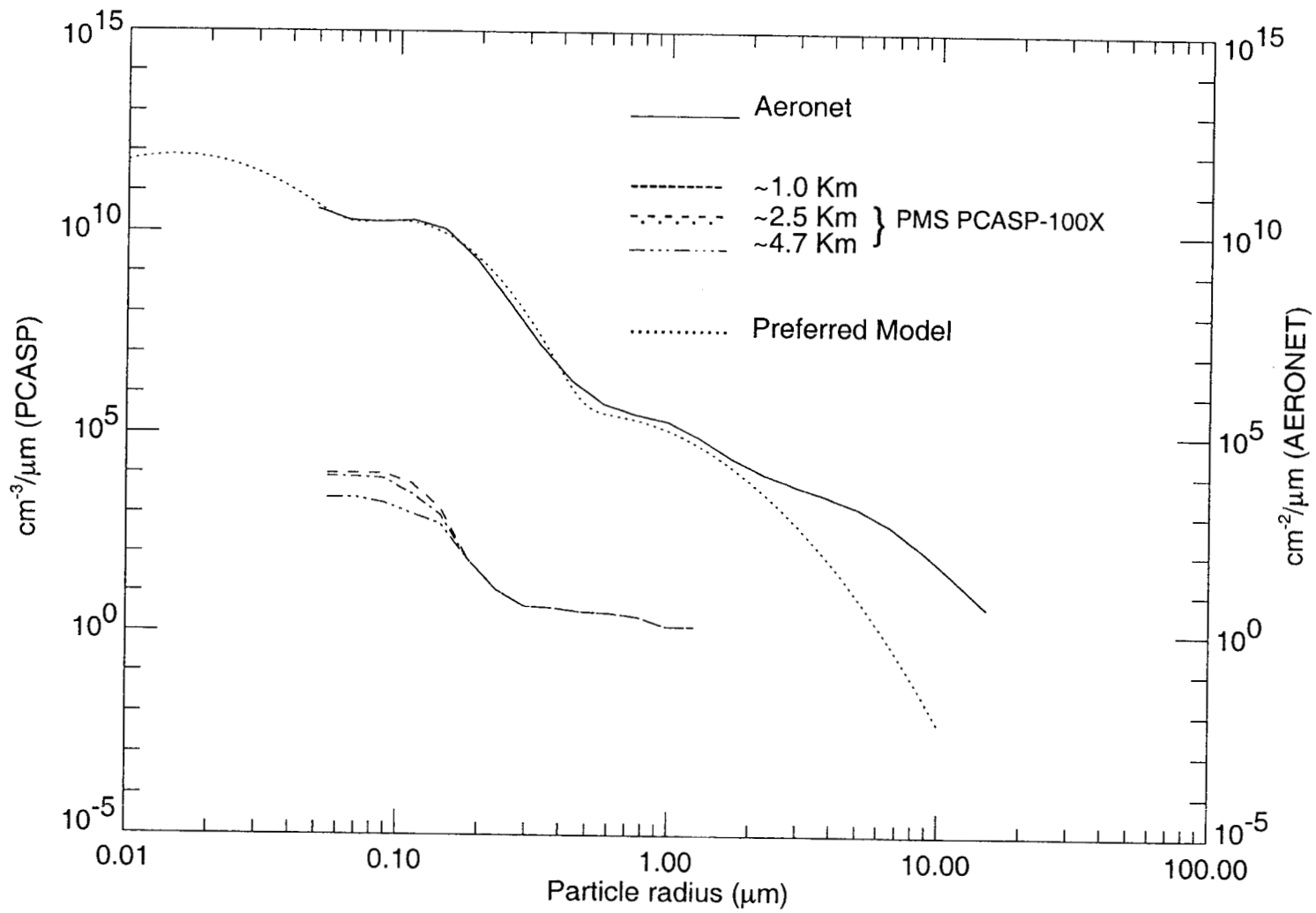


Figure 8.

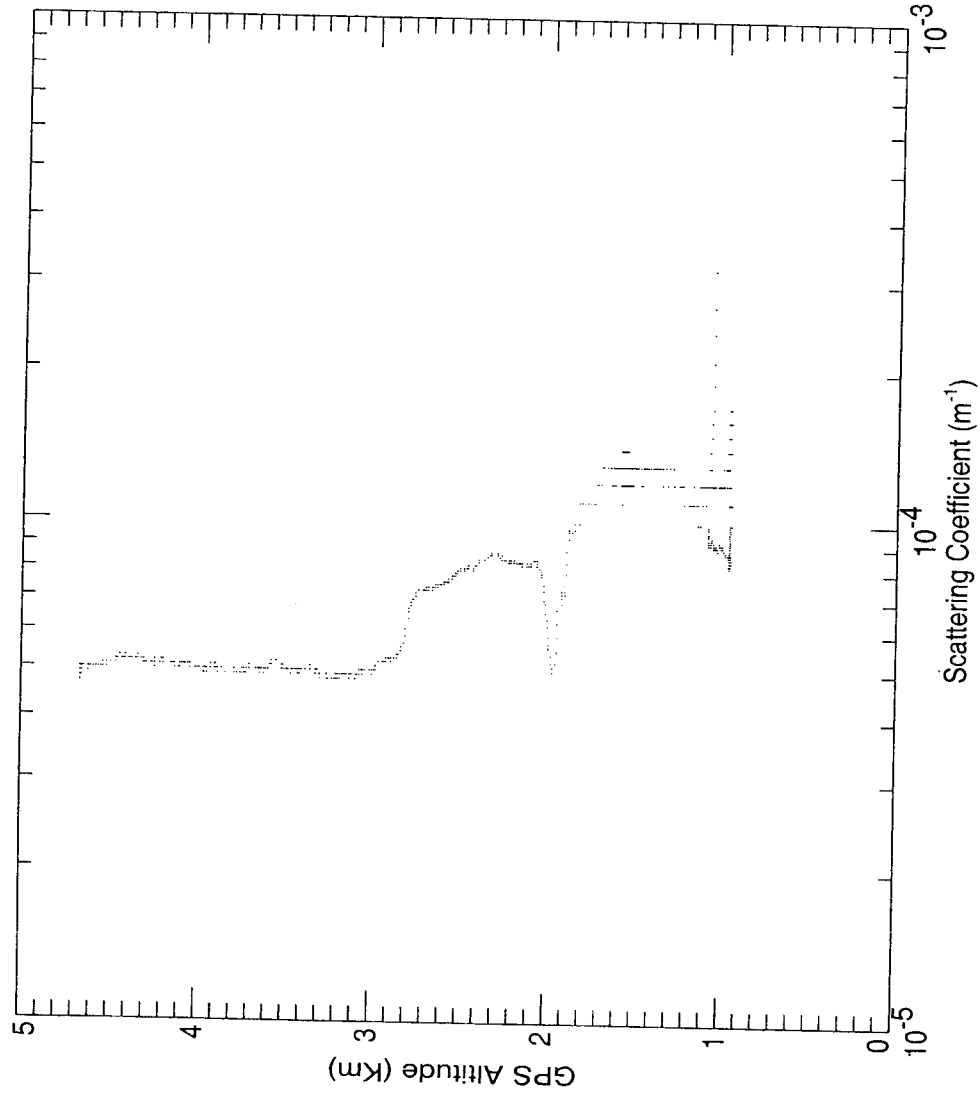


Figure 9.

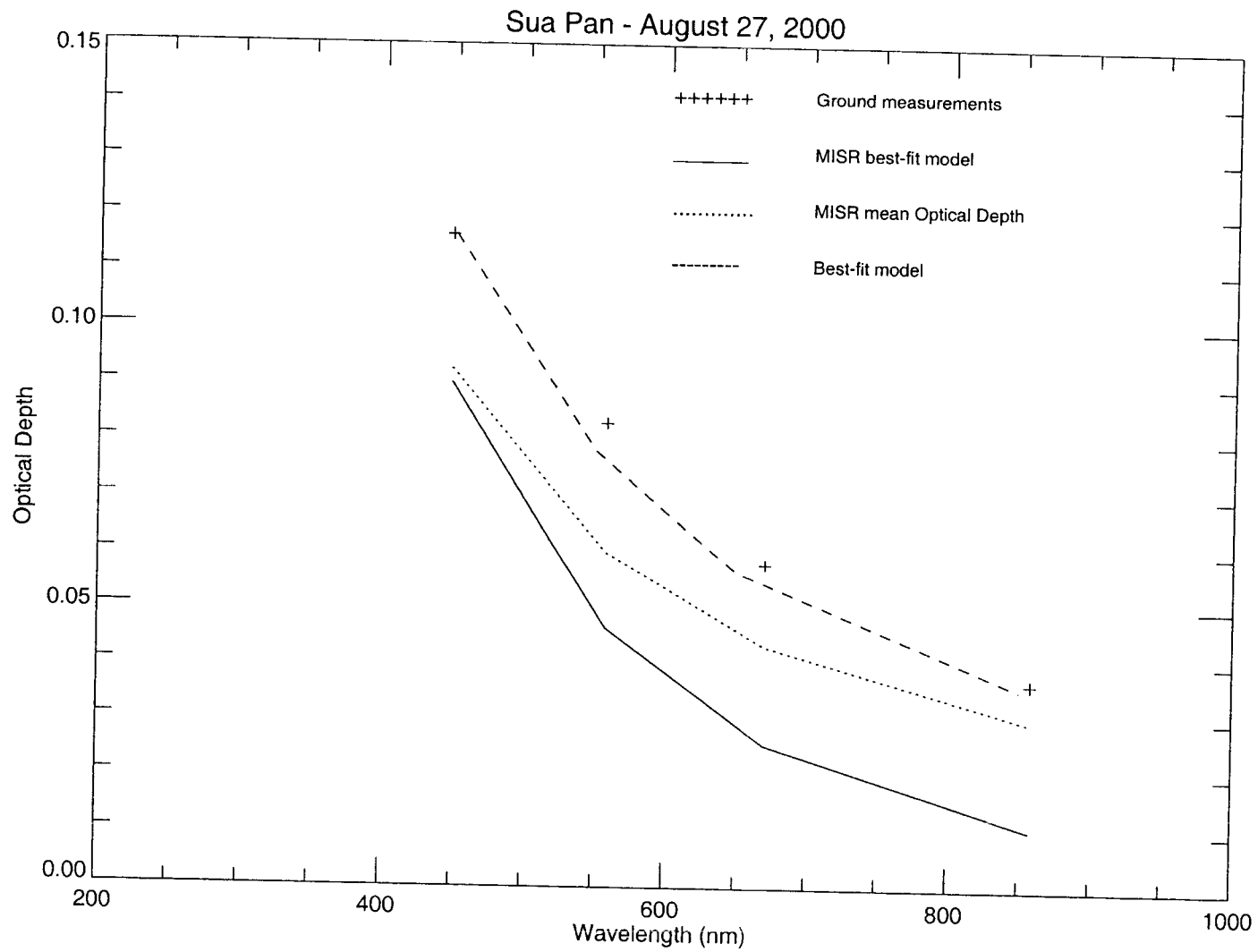


Figure 10.

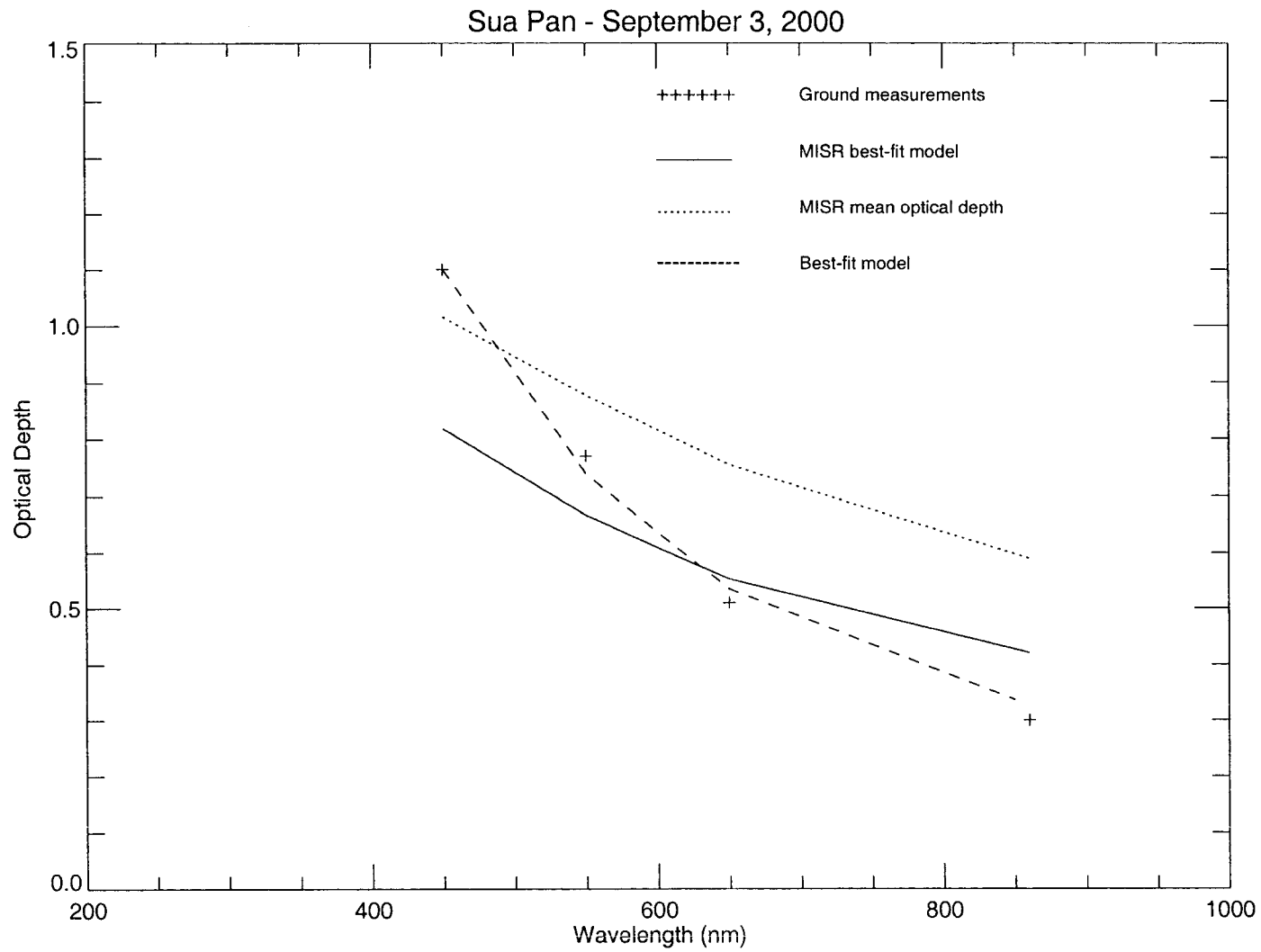


Figure 11.

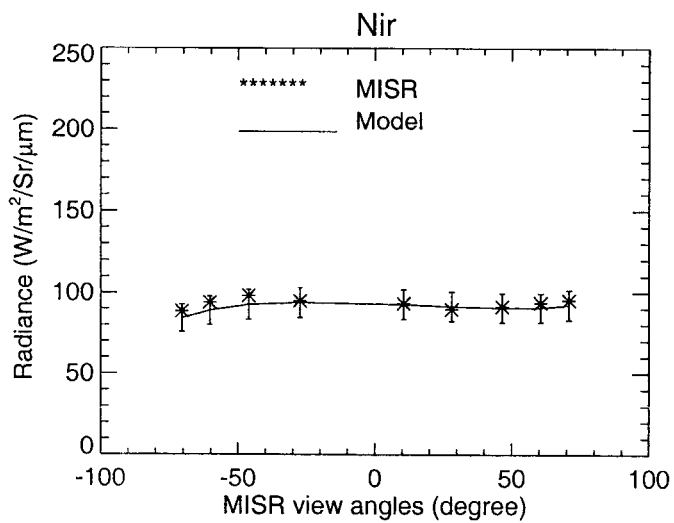
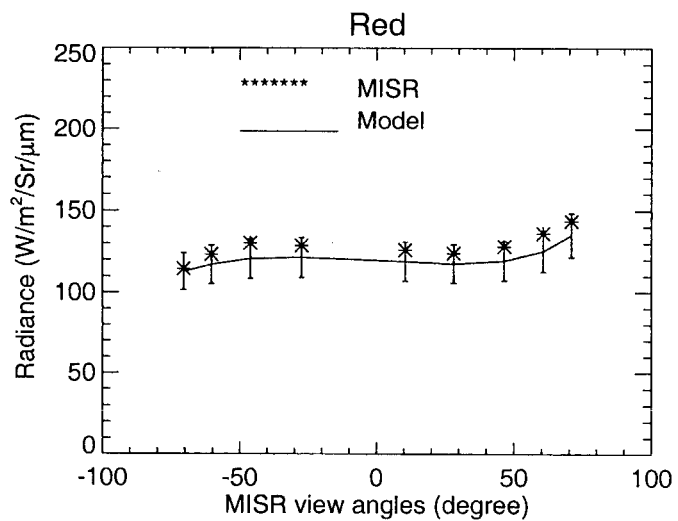
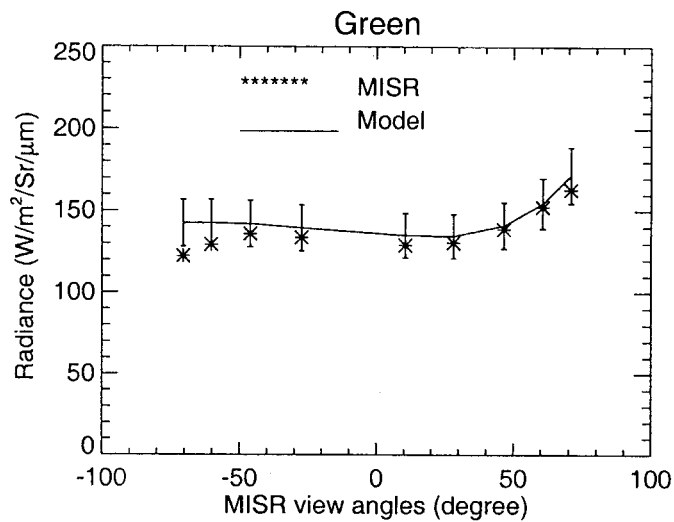
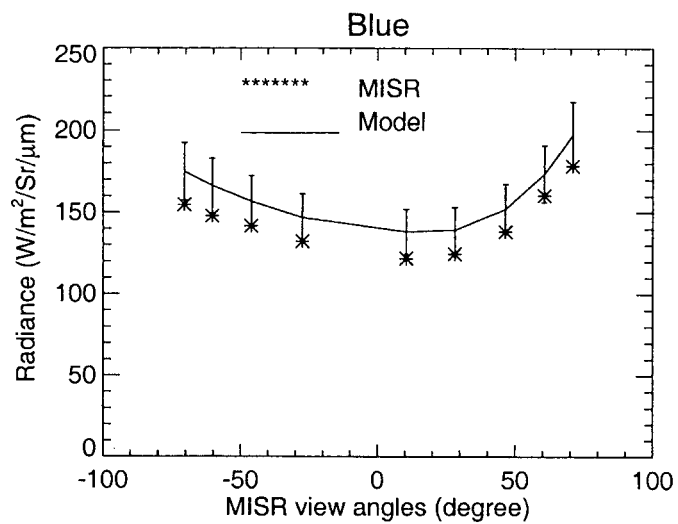


Figure 12